AD-766 961

DISCRIMINATION AMONG SMALL MAGNITUDE EVENTS ON NEVADA TEST SITE

William A. Peppin, et al

California University

Prepared for:

Air Force Office of Scientific Research

August 1973

Discrimination among Small Magnitude Events on Nevada Test Site

Wm. A. Peppin

T. V. McEvilly

Seismographic Stations
Department of Geology and Geophysics
University of California
Berkeley, California

UNCLASSIFIED

Security Classification

DOCUMENT CONTROL DATA - R & D

(Security classification of title, body of abstract and indexing annotation must be entered when the overall report is classified)

1. ORIGINATING ACTIVITY *(Corporate author)*

University of California, Berkeley
Department of Geology and Geophysics
Berkeley, CA 94720

2a. REPORT SECURITY CLASSIFICATION

UNCLASSIFIED

2b.

3. REPORT TITLE

Discrimination Among Small Magnitude Events on Nevada Test Site

4. DESCRIPTIVE NOTES *(Type of report and inclusive dates)*

Scientific.....Interim

5. AUTHOR(S) *(First name, middle initial, last name)*

Wm. A. Peppin and T. V. McEvilly

6. REPORT DATE	7a. TOTAL NO. OF PAGES	7b. NO. OF REFS
August 1973	26 29	28

8a. CONTRACT OR GRANT NO.	9a. ORIGINATOR'S REPORT NUMBER(S)
AFOSR-73-2563	
b. PROJECT NO. AO 1827-7	
c. 62701E	9b. OTHER REPORT NO(S) *(Any other numbers that may be assigned this report)* AFOSR - TR - 73 - 1586
d.	

10. DISTRIBUTION STATEMENT

Approved for public release; distribution unlimited.

11. SUPPLEMENTARY NOTES	12. SPONSORING MILITARY ACTIVITY
TECH, OTHER	Air Force Office of Scientific Research/NPG 1400 Wilson Boulevard Arlington, VA 2209

13. ABSTRACT

Broadband data (.02 to 20 Hz) from the University of California Lawrence Livermore Laboratory four-station seismic array, deployed at close range (less than 500 km) azimuthly about Nevada Test Site (NTS), allow investigation of the body wave-surface wave discriminant between explosion and earthquakes for small events confined to NTS, extending previous results to magnitudes (M_L) around 3.5. It is found that natural earthquakes, explosion collapses, and explosion aftershocks all are distinct from explosions, and that the populations do not seem to converge at the low magnitudes. Also, for explosions, there is no change in the slope of the P_n versus Rayleigh wave amplitude relation over more than three orders of magnitude. Since the non-explosion events are shallow, of low magnitude, and of different source types, differences in source dimension, focal depth, and focal mechanism appear inadequate to explain the discriminant at small magnitudes.

DD FORM 1 NOV 65 1473

UNCLASSIFIED

Security Classification

ABSTRACT

Broadband data (.02 to 20 Hz) from the University of California Lawrence Livermore Laboratory four-station seismic array, deployed at close range (less than 500 km) azimuthally about Nevada Test Site (NTS), allow investigation of the body wave-surface wave discriminant between explosion and earthquakes for small events confined to NTS, extending previous results to magnitudes (M_L) around 3.5. It is found that natural earthquakes, explosion collapses, and explosion aftershocks all are distinct from explosions, and that the populations do not seem to converge at the low magnitudes. Also, for explosions, there is no change in the slope of the P_n versus Rayleigh wave amplitude relation over more than three orders of magnitude. Since the non-explosion events are shallow, of low magnitude, and of different source types, differences in source dimension, focal depth, and focal mechanism appear inadequate to explain the discriminant at small magnitudes.

INTRODUCTION

In this paper the broadband data of the University of California Lawrence Livermore Laboratory (LLL) seismic array are used to study P-waves and Rayleigh waves generated by Nevada Test Site (NTS) events at low magnitudes. The study was planned to extend the work of McEvilly and Peppin (1972), which used Berkeley data, to smaller magnitude events, all on NTS, with azimuthal observations available. Data from 56 events are analysed as recorded at the four LLL stations deployed around NTS, both with regard to P-wave and Rayleigh wave amplitudes and with regard to P-wave spectra. Motivation for the investigation is straightforward: we have in the LLL array an unequalled tool to study the body wave-surface wave discriminant for NTS at low magnitudes. Further, we would like to consider the applicability of the discrimination results obtained here to other regions. Toward this end we search for possible peculiarities in NTS earthquakes making them unusually easy to discriminate from explosions at NTS.

THE LLL SEISMIC NETWORK

The LLL broadband seismic array, in operation since late 1968, consists of the four stations shown in Figure 1. Outputs from vertical seismometers operating at natural periods of either 20 or 30 seconds are telemetered to Livermore, California and recorded on magnetic tape at three gain levels with 20 dB separations. Response curves for the LLL seismometer-tape system at maximum sensitivities are shown in Figure 2 along with that of the Berkeley tape system for comparison. In addition, remotely controlled amplifiers at the seismometer can be varied by 60 dB,

and are set prior to explosions at levels chosen to produce full scale recording of these events on the medium gain channel. Except at times of explosions, the amplifiers are normally set six dB below the sensitivities shown in Figure 2. The threshold for measurable ground motions at normal operating gains are about 40 and 5 nanometers (nm) of peak-to-peak ground displacement in the 12 second Rayleigh and short period P_n phases respectively, a factor of five to ten times smaller than obtained with the Berkeley tape system. Careful analysis of the curves in Figure 2 would imply a greater difference, even at the -6dB level on LLL stations. The discrepancy lies in a difference of 2 to 4 in dynamic range of the tape systems used.

DATA AND PROCEDURE

The 56 events chosen for this study are all within NTS. An effort has been made to include the smallest events that have occurred since late 1968 when the LLL network began operation, but for various reasons not all are included. As in the previous study, amplitudes of the Rayleigh wave and P_n wave were read to obtain their relation (analogous to but not exactly equivalent to the M_s:m_b plot commonly constructed at teleseismic distances). The long period measurement was taken to be the 12 second Rayleigh wave amplitude, taken from a filtered (.02-.1 Hz, 48 db per octave) tape system playout. The severe filtering was used to suppress the 6 second microseisms, which on the unfiltered playouts were often within 6 dB of full scale on the high gain channel. The short period measurement was maximum P_n amplitude, hereinafter designated "PNMAX", taken from a filtered (.5-5Hz, 24 db per octave) playout. For explosions the frequencies measured were 2-4 Hz, with most near 2.5 Hz, over the entire magnitude range (with important excep-

tions noted below); for earthquakes and collapses the ranges of frequencies measured were 2-3 Hz and 0.75-1.5 Hz, respectively. Attempts were made to use other short period measurements, for example the first swing of P_n, hereinafter designated "PN1", and P_g maximum amplitude. For explosions each of these gave plots with small scatter, but for non-explosions, the P_g data were badly scattered, and PN1 was not readable for the smallest of these. PNMAX was selected for comparison with the Rayleigh amplitude because it gives the least scatter and the phase itself has the most uniform appearance over the wide range of magnitudes studied.

Events analyzed, with amplitude measurements, are given in Table 1. Amplitudes are uncorrected for attenuation and geometric spreading as the variation in distance is small (less than 50 km). One unit represents peak-to-peak ground displacements of about 4 nm and 0.5 nm for the 12 second Rayleigh wave and 2-4 Hz P_n wave , respectively. Readings considered upper bounds due to signal/noise levels are so indicated. Also given in Table 1 are local magnitudes, M_L. For all the events above $M_L = 4.0$ these are based on Wood-Anderson readings at Berkeley. For smaller events, the Berkeley M_L value is based extrapolation of the scale to high gain short period vertical data as routinely done for small California earthquakes.

This study improves upon our previous work (McEvilly and Peppin, 1972) in a number of respects: (1) the data consist of NTS events only, so that source region and propagation path are much less variable; (2) we have azimuthal coverage, so that the influence of station site, propagation path, and earthquake focal mechanism on the discriminant can be evaluated; (3) because of higher magnification and closer proximity to NTS, events nearly a magnitude unit smaller can be studied; (4) both measurements are made

on the same instrument; and (5) each explosion receives optimal recording, because the sensitivity is adjusted to match the expected signal.

RESULTS

In Figure 3 we present the data taken at Elko, Nevada. Plotted are PNMAX versus 12 second Rayleigh amplitude from Table 1. In this and the three subsequent figures, three categories of non-explosion events are designated. "Explosion aftershocks" are events occurring shortly after and in the vicinity of large NTS explosions, but which are not "collapses". "Collapses" are distinctive sources, characterized by their relatively emergent, long period P arrivals and phase reversal of surface waves relative to the causative explosion (McEvilly and Peppin, 1972). "Earthquakes" are events apparently unrelated to explosions. In Figures 3-6 the readings from Table 1 considered as upper bounds are so indicated. With the limited data of Figure 3, explosions and earthquakes appear separated at the low magnitude end.

In Figure 4 data from Kanab, Utah are shown. We see clear separation of explosions from all other events, and parallel population trends. For confident discrimination purposes though, the differences would not be sufficient.

In Figure 5 are shown the Landers, California data. Again we have separation, but not by a large margin. Event #37, an explosion aftershock, is anomalous at Landers because it plots outside the explosion population in several other data sets: at three other LLL stations; on the Berkeley broadband system (McEvilly and Peppin, 1973); and in Basham's (1971) study of NTS aftershocks.

In Figure 6 are the Mina, Nevada data. Here we find definitive separation of explosions from all but one of the other events. The exceptional

collapse, event #54, is distinct from explosions at the other three LLL stations and at Berkeley. The Mina arrivals for this event are, however, unmistakably of collapse type in character, despite their numerical values.

As in our previous study using BRK data from similar instrumentation, the limitations at the low magnitude end of the data set are different for explosions than for the other events. The detection threshold for useable explosion data is set by the Rayleigh wave vanishing into the noise level below about 40 nm peak-to-peak amplitude (P_n readings could be made for explosions nearly another order of magnitude smaller). Non-explosion events, however, are limited by disappearance into background of the P_n wave at some 5 nm peak-to-peak amplitude, while the associated Rayleigh waves are still clearly detectable. Other than analog filtering, no signal enhancement techniques were applied to the data.

DISCUSSION

A. The Discriminant at Low Magnitudes

The most important result in the data of Figures 3-6 is the extension to low magnitudes of the clear separation of explosions from other events. The Mina data suggest that this separation can be extrapolated perhaps a magnitude unit lower than the smallest explosions shown in Figure 6. For comparison with previous results, we note that the smallest explosions for which surface waves can be read in the studies of Savino *et al* (1971), Basham *et al* (1971), and McEvilly and Peppin (1972) are, respectively, of magnitudes M_L 5.0, 4.5 and 4.2. These compare with Event #13, of $M_L = 3.6$ in this study. Local magnitude was found (McEvilly and Peppin, 1972) to relate to body wave magnitude (Savino, *et al*, 1971) as $m_b' \simeq M_L - 0.4$ at M_L o 4.0.

B. Possible Causes of the P_n vs. Rayleigh Discriminant

We consider first the possibility of differences in spatial source dimension causing the discriminant. To this end, we assume, based on the theories of Haskell (1964), Aki (1967) or Brune (1970) that the far-field spectra of seismic P-waves can be characterized by a flat section at low frequencies, extending to a corner frequency, f_c, which is proportional to spatial source dimension, and at higher frequencies a decay rate greater than inverse frequency squared.

Elementary considerations of the interference effects due to a finite source would lead to a corner frequency dependence of the form

$$f_c \propto \frac{C}{L}$$

where C and L are wave velocity at the source and maximum soure dimension as viewed from the observation point, respectively. The constant of proportionality is unity by simplistic arguments, and $2.34/\pi$ for S-waves according to Brune (1970) or as extended to P-waves by Hanks and Wyss (1972).

Source dimensions for small magnitude events can be estimated from extrapolation of data of Tocher (1958), Iida (1959) and Press (1967), yielding a maximum dimension of 0.2 km at $M_L = 3.0$. Wyss and Brune (1968) predict a fault length around 1 km at this magnitude.

For the above ranges of dimensions and proportionality constants, and for C = 5 to 6 km/sec, the minimum value of f_c for $M_L = 3.0$ is estimated as 4 to 30 Hz. In the sense of gross spectral characteristic, then, both the Rayleigh and P_n measurements for the smallest earthquakes in this study are made on the low frequency flat parts of their amplitude spectra.

For explosions, Springer and Hannon (1973) find that explosion-yield

data are best explained by far-field displacement spectra that are flat from low frequency to a corner frequency, which, for a source of 5 kilotons in tuff ($M_L \simeq 4.1$) occurs around 3 Hz. On this basis the Rayleigh and P_n measurements for the smallest explosions used in this study appear also to be made on the low frequency flat parts of their spectra.

The argument follows that, since measurements for explosions and earthquakes at the low magnitude levels are made at frequencies low relative to the frequencies affected by source dimensions, then the existence of a clear discriminant for the smallest events considered precludes source dimension differences as a major causal factor. Furthermore, the parallel, linear Rayleigh-P_n relations seen for explosions and earthquakes for the range $M_L < 4$ to $M_L > 6$ (McEvilly and Peppin, 1972, also) would indicate that source dimension differences do not become a significant factor in the discriminant at larger magnitudes either.

Focal mechanism has been suggested by several authors (Tsai and Aki, 1971; Douglas et al 1971 a,b) as a cause of the $M_S - m_b$ discriminant, essentially equivalent to the P_n vs Rayleigh discriminant here. In this connection, we note that Events 35, 36, and 37 are dip-slip earthquakes while Events 30, 31, 33, 40, 41, and 42 are strike-slip and have fault planes whose strikes vary by more than twenty degrees (Hamilton, personal communication, 1970; Fischer et al, 1972; Fischer personal communication, 1973). Yet no influence on the data of Figures 4-6 can be seen, in spite of considerable variations in surface wave excitation expected theoretically from these sources. Therefore, focal mechanism appears not to be a dominant factor, although this point needs further study.

Focal depth differences can hardly be a major factor in the cause of

the discriminant. Collapse events have hypocenters identical to their causative explosions. Moreover, the earthquakes and explosion aftershocks have quite shallow focal depths, 4.6, 4.7, 3.5, 2.1, 2.7, and 3.6 km respectively for Events 30, 33, 36, 39, 40 and 43 (Fischer personal communications, 1970, 1973, Fischer et al, 1972).

The source time function remains as probably the most significant causal parameter for the discriminant, in part because of the strong grounds for eliminating other contenders. This possibility has been suggested recently by a number of authors: Liebermann and Pomeroy (1968), Marshall (1970), Savino et al (1971), for example. The close similarity (apart from a phase reversal) of the collapse Rayleigh wave to that from its causative explosion, though they differ in size by two or more orders of magnitude and are presumably of similar small spatial source dimension, supports a source time function difference for their clear separation. This separation is well observed in the LLL data, particularly in the collapse sequences of JORUM and HANDLEY, several of which appear in Table 1. Rise-time characteristics of the source time function, as for spatial source dimension, will introduce another corner on the far-field displacement spectrum (Haskell, 1964), with a high frequency rolloff slope dependent on the order of differentiability of the rise time function. If explosions are characterized by sharper rise times than earthquakes, the discriminant can arise if the time function corners are at lower frequencies for earthquakes and at higher frequencies for explosions than the frequencies measured. Such a simple explanation is undoubtedly deficient, because the short period-long period discriminant obtains for a range of

short period frequencies measured (2-5 Hz in this study, and less than 1 Hz at teleseismic distances). However, basic differences in P-spectra are indicated by the success of short period spectral ratios in P-wave discriminants.

C. Short Period vs. Long Period Trend for Explosions

Springer and Hannon (1973) have presented data on P_n versus Rayleigh amplitude for explosions that show a quite linear relationship over three orders of magnitude, in contrast to the data of Evernden and Filson (1971) and the theory of Tsai (1972), plus many other studies of explosion seismic scaling based on Sharpe's (1942) solution for a pressure pulse in a spherical cavity and observed reduced displacement potentials as in Werth and Herbst (1963) (a bibliography of such studies can be found in Springer and Hannon (1973)). Unfortunately our previous work (Evernden, et al, 1971, McEvilly and Peppin, 1972), presents a plot that could be interpreted as indicating a change in slope of the explosion line for M_L below 4.5. As was pointed out by McEvilly and Peppin (1972), however, the small explosions used represented generally those with the largest Rayleigh waves in the magnitude range, frequently readings just at noise levels and possibly overestimated, biasing the explosion line toward larger Rayleigh wave values at small magnitudes. The apparent indication of a change in slope at small magnitudes is an artifact of such bias. In this study such upper bound data points are indicated clearly in Figures 3 to 6.

The explosion data of Mina, Kanab, and Landers were fit by the method of least squares to the line

$$\log R = k \log P + b$$

where R is the Raylelgh amplitude from Table 1 and P is either PNMAX from Table 1 or PN1. The slopes, k, and estimates of their standard errors (Hald, 1952, p. 540) are shown in Table 2, along with the number of data points, equally weighted, in parentheses. Data from McEvilly and Peppin (1972) and Springer and Hannon (1973) are included for comparison. Note that the PN1 slope taken from Springer and Hannon (1973) was not published by them because their data failed to pass a statistical acceptance test as being one group. Only the data for the explosions which appear in Figures 4-6 were included in the respective regression analyses. We note that at all the LLL stations the frequencies at which PN1 were measured were 3-5 Hz (vs 2-4 for PNMAX). The slopes for PN1 are smaller than those for PNMAX, but it is difficult to say if these variations are significant, despite the relatively small uncertainties on the slopes. If significant, the variation may be due to either the slightly different frequencies measured, or to the propagation paths, including effects of any systematic depth-yield linearity. Since the same effect appears in the data of Springer and Hannon in Table 2, we conclude that these small differences in frequency content are at least partially responsible for the differences in slope. Basically, this observation implies that PNMAX increases with increasing Rayleigh amplitude more slowly than does PN1, which goes close to 1:1.

We now extrapolate the regression lines of Table 2 to larger magnitudes in order to consider the large explosions JORUM and HANDLEY (Table 1) which were not used in the regression analysis. In Table 3 we list the deviations in standard error units of the JORUM and HANDLEY measurements from the extrapolated lines. A positive value means that the point lies

above the extrapolated regression line, i.e., relatively more Rayleigh wave than predicted by extrapolation from smaller explosions. Included in parentheses are the frequencies in Hz at which the phases are measured.

Of the data in Table 3, only the PNi measurements at Mina and Kanab are similar in frequency and waveform to the measurements for all other explosions in Table 1. These points fall close to the extrapolated regression lines from smaller explosions. We therefore conclude that similarly measured P_n versus Rayleigh wave data for explosions can be described by a line of constant slope over almost four orders of magnitude. This is in agreement with work of Springer and Hannon (1973). It also implies that 3-5 Hz P_n waves and 12 second Rayleigh waves have virtually identical scaling relations to yield, including any slope changes, over this magnitude range.

D. A Peculiar Nature of NTS Earthquakes?

To explore the generality of the above results we apply the P-wave spectral theory of Hanks and Wyss (1972) to determine if NTS earthquakes are anomalous excitors of surface waves. Displacement spectra were computed for the main Pg phase of four events with high signal-to-noise ratios (20 to 30 seconds of data, 50 samples per second, 10% cosine taper) and source parameters were estimated as follows:

$$M_o = \frac{4\pi\rho R\alpha^3\Omega_p}{R_{\theta\phi}}$$

$$r = \frac{2.34\alpha}{2\pi f_c}$$

$$\sigma = \frac{7}{16}\frac{M_o}{r^3}$$

The quantities above are those defined by Hanks and Wyss (1972). The long period part of the spectrum of the P_g phase spectrum was estimated, along with the corner frequency as illustrated in Figure 7. The radiation pattern term $R_{\theta\phi}$, the density ρ, and the P-velocity α were taken as 0.4, 2.7, and 5.5×10^5 cgs, respectively, with source parameters M_o, r and σ estimated as indicated. Results appear in Table 4. The small stress drops, σ , are consistent with those found by Douglas and Ryall (1972) for small central Nevada earthquakes. The three explosion aftershocks fall on or below the curve $\log M_o = 1.7\ M_L + 5.1$ found by Wyss and Brune (1968) to fit Western U.S. earthquakes, while the natural earthquake of 05 August 1971 (event 30) falls above the curve (relatively more moment for a given magnitude). According to the theory of Douglas et al, (1971a), we should expect more excitation of surface waves relative to body waves for shallower earthquakes. The spectral data of Table 4 imply that NTS earthquakes should generate surface waves relative to their magnitude comparable to those of other Western U.S. earthquakes. But, since the focal depths of the NTS events are quite shallow relative to other Western U.S. earthquakes (Table 1), we cannot conclude from these data that the low magnitude P_n - Rayleigh discriminant documented in Figures 3 to 6 would obtain at any other Western U.S. test site. Again we point out, however, that focal depth may be unimportant; event 31 is small and otherwise not unlike other events in Figs. 3-6 in spite of its considerably greater focal depth (Table 1).

Conclusions

The short period-long period, or body wave-surface wave discriminant

between explosions and other events on NTS is well-documented down to M_L = 3.3, and appears to extend to M_L less than 3. Focal depth and spatial source dimension seem unlikely as the prime cause of the discriminant at small magnitudes, focal mechanism less definitely so, and the source time function seems to be the most likely causal parameter. A plot of log P_n amplitude versus Rayleigh amplitude for explosions is well described by a straight line in the range $3.6 \leq M_L \leq 5.2$, but the slope of the line is a function of the frequencies measured and of the stations where the measurements are made (values here obtained vary from 1.01 ± .045 to 1.32 ± .051). Since NTS events do not appear to be exceptional excitors of surface waves relative to other Western U.S. earthquakes, these results can be generalized perhaps to that region.

ACKNOWLEDGMENTS

We are indebted to D. L. Springer of the University of California Lawrence Livermore Laboratory for assistance in acquiring raw data basic to this study and to R. M. Hamilton and F. Fischer of the National Center for Earthquake Research for details of NTS aftershocks and earthquakes. This research was supported by the Advanced Research Projects Agency of the Dept. of Defense and was monitored by the Air Force Office of Scientific Research under Grants No. AFOSR-69-1783, AFOSR-72-2392, and AFOSR-73-2563.

BIBLIOGRAPHY

Akl, K., 1967. Scaling Law of Seismic Spectrum, Jour. Geoph. Res., 72, 1217-1231.

Basham, P. W., 1969. Canadian Magnitudes of Earthquakes and Nuclear Explosions in Southwestern North America, Geoph. J. R. A. S., 17, 1-14.

Brune, J. N., 1970. Tectonic Stress and the Spectra of Seismic Shear Waves from Earthquakes, Jour. Geoph. Res., 75, 4997-5010.

Douglas, A.,, Hudson, J. A., and Kembhavi, V. K., 1971a. The Relative Excitation of Seismic Surface and Body Waves by Point Sources, Geoph. J.R.A.S., 23, 451-460.

Douglas, A., Hudson, J.A., and Kembhavi, V.K., 1971b. The Analysis of Surface Wave Spectra Using a Reciprocity Theorem for Surface Waves, Geoph. J.R.A. S., 23, 207-223.

Douglas, Bruce M. and Ryall, Alan, 1972. Spectral Characteristics and Stress Drop for Microearthquakes Near Fairview Peak, Nevada, Jour. Geoph. Res., 77, 351-359.

Evernden, J.F., Best, W.J., Pomeroy, P.W., McEvilly, T.V., Savino. J.M. and Sykes, L.R., 1971. Discrimination between Small-Magnitude Earthquakes and Explosions, Jour. Geoph. Res., 76, 8042-8055.

Evernden, J.F. and Filson, John, 1971. Regional Dependence of Surface-Wave Versus Body Wave Magnitudes, Jour. Geoph. Res., 76, 3303-3308.

Fischer, F.G., Papanek, P.J. and Hamilton, R.M., 1972. The Massechusetts Mountain Earthquake of 5 August 1971 and its Aftershocks, Nevada Test Site, U.S.G.S Paper 474-149.

Hald, A., 1952. Statistical Theory with Engineering Applications, John Wiley and Sons, New York.

Hamilton, R.M., Smith, B.E., Fischer, F.G. and Papanek, P.J., 1971. Seismicity of the Pahute Mesa Area, Nevada Test Site, 8 Dec 1968 throuth 31 Dec 1970, Special Studies 89, U.S.G.S. Paper 474-128.

Hanks, Thomas C. and Wyss, Max, 1972. The Use of Body-Wave Spectra in the Determination of Seismic Source Parameters, Bull. Seism. Soc. Am., 62, 56;-589.

Haskell, N.A., 1964. Total Energy and Energy Spectral Density of Elastic Wave Radiation from Propagating Faults, Bull. Seism. Soc. Am., 54, 1811-1841.

Ilda, K., 1959. Earthquake Energy and Earthquake Fault, Jour. Earthquake Sci. Nagoya Univ., 7, 98-107.

Liebermann, Robert C., and Pomeroy, Paul W., 1969. Relative Excitation of Surface Waves by Earthquakes and Underground Nuclear Explosions, Jour. Geoph. Res., 74, 1575-1590.

Marshall, P.D., 1970. Aspects of the Spectral Differences Between Earthquakes and Underground Nuclear Explosions, Geoph. J.R.A.S., 20, 397-416.

McEvilly, T.V. and Peppin, W.A., 1972. Source Characteristics of Earthquakes, Explosions, and Afterevents, Geoph. J.R.A.S., 31, 67-82.

Press, Frank, 1967. Dimensions of the Source Region for Small, Shallow Earthquakes, Proceedings of the VESIAC Conference on the Current Status and Future Progress for Understanding the Source Mechanism of Shallow Seismic Events in the 3 to 5 Magnitude Range.

Savino, J., Sykes, L.R., Liebermann, R.C. and Molnar, P. 1971. Excitation of Seismic Surface Waves with Periods of 15 to 70 Seconds from Earthquakes and Underground Explosions, Jour. Geoph. Res., 76, 8003-8020.

Sharpe, J.A., 1942. The Production of Elastic Waves by Explosion Pressures, 1. Theory and Empirical Field Observations, Geoph., 7, 144-154

Springer, Donald L. and Hannon, Willard J., 1973. Amplitude-Yield Scaling for Underground Nuclear Explosions, Bull. Seism. Soc. Am, 63, 477-500.

Springer, Donald L. and Kinnaman, Ross L., 1971. Seismic Source Summary for U.S. Underground Nuclear Explosions, 1961-1970, Bull. Seism. Soc. Am, 61, 1073-1098.

Thatcher, Wayne and Hanks, Thomas C., 1973. Source Parameters of Southern California Earthquakes, in press, 1973.

Tocher, Don, 1958. Earthquake Energy and Ground Breakage, Bull. Seism. Soc. Am., 48, 147-153.

Tsai, Yi-Ben, 1972. Utility of Tsai's Method for Seismic Discrimination, Advanced Research Project Agency Semi-Annual Technical Report no. 2, 1 Jan 1972 to 30 Jun 1972.

Tsai, Yi-Ben and Aki, Keiiti, 1971. Amplitude Spectra of Surface Waves from Small Earthquakes and Underground Nuclear Explosions, J. Geoph. Res., 76, 3940-3952.

Werth, G.C. and Herbst, R.F., 1963. Comparison of Amplitudes of Seismic Waves from Nuclear Explosions in four Mediums, J. Geoph. Res., 68, 1463-1475.

Wyss, Max and Brune, James N., 1968. Seismic Moment, Stress, and Source Dimensions for Earthquakes in the California-Nevada Region, J. Geoph. Res., 73, 4681-4694.

TABLE 1. Data on Events Used

Event No.	Date	Type	T_o (GMT)	Lat. (N)	Long. (W)	Depth (km)	AMPLITUDES ELKO R	ELKO PNMAX	KANAB R	KANAB PNMAX	LANDERS R	LANDERS PNMAX	MINA R	MINA PNMAX	M_L	Source
1*	18 Sep 69	JORUM	EX 14 30 00	37°18.9'	116°27.6'	1.2					41000	18000	95000	40000	8.2	(1)
2	29 Oct 69	CHUET	EX 19 30 00	37°07.4'	118°07.7'	.2			44	208	30	74	44	328	4.4	(1)
3	29 Oct 69	FOD	EX 20 00 00	37°08.1'	114°08.1'	.3			105	320	60	240	175	460	4.6	(1)
4	29 Oct 69	CALABASH	EX 22 01 52	37°08.6'	114°03.8'	.9					2800	1920			5.5	(1)
5	25 Feb 70	CUSHAWS	EX 14 28 38	37°02.2'	118°00.0'	.4			750	1200			850	1340	4.6	(1)
8	28 Feb 70	YAMNIGAN	EX 15 30 00	37°07.0'	114°03.7'	.4			350	800			600	1400	4.8	(1)
7	06 Mar 70	CYATHUS	EX 14 24 01	37°01.4'	116°05.5'	.3			17	60	40	70	105	180	4.2	(1)
8	06 Mar 70	ARABIS	EX 15 00 00	37°08.4'	116°02.2'	.2			7	26	<25	35	<15	140	4.1	(1)
9	19 Mar 70	JAL	EX 14 03 30	37°00.1'	116°01.4'	.3			<30	150			70	148	4.1	(1)
10	23 Mar 70	SHAPER	EX 23 05 00	37°05.2'	116°01.3'	.5			2700	4200	2500	1500	2800	6000	5.4	(1)
11*	28 Mar 70	HANDLEY	EX 19 00 00	37°18.0'	116°32.0'	1.2			90000	28400	48000	27200	110000	50000	6.2	(1)
12	15 May 70	CORNICE	EX 13 30 00	37°09.7'	116°02.3'	.4			1200	840	950	440	1200	4880	5.0	(1)
13	21 May 70	MANZANAS	EX 14 00 00	37°01.7'	115°59.5'	.3			30	188			13	44	3.6	(1)
14	21 May 70	MORRONES	EX 14 15 00	37°04.3'	116°00.7'	.4	400	850	900	1600	600	550	800	1700	5.0	(1)
15	28 May 70	HUDSON MOON	EX 14 16 00	37°11.0'	116°12.8'	.4			29	140	42	116	150	560	4.2	(1)
16+	24 May 70	FLASK	EX 15 00 00	37°06.8'	116°03.7'	.5					1700	550	2200	4900	5.2	(1)
17+	28 May 70		EX 12 00 03	37.2°	116.0°	<1			30	105	<24	38	<15	70	3.9	(3)
18	18 Jun 71	RUDD	EX 14 50 00	37° 02.0'	116°00.8'	<1			60	220	80	100			4.2	(2)
19	23 Jun 71	LAGUNA	EX 15 30 00	37°01.3'	116°01.4'	<1	220	320	190	1300	300	480	660	1250	4.5	(2)
20	24 Jun 71	MARRSELL	EX 14 00 00	37° 08.8'	116°04.0'	<1	350	760	500	760	450	380	560	1240	4.9	(2)
21+	29 Jun 71		EX 18 30 00	37°	116°	<1			300	1720			600	1160	4.4	(3)
22+	22 Sep 71		EX 14 00 00	37°	116°	<1			<20	45	25	38	<15	48	3.9	(3)
23	29 Sep 71	PEDERNAL	EX 14 00 00	37°00.4'	116°00.4'	<1			100	400			156	720	4.1	(2)
24+	08 Oct 71	CATHAY	EX 14 30 00	37°06.8'	116°02.3'	<1	110	200	126	440	90	180	124	400	4.7	(2)
25+	14 Oct 71		EX 14 30 00	37.2°	116.1°	<1							110	530	3.9	(3)
26+	30 Nov 71		EX 15 45 00	37.1°	116.1°	<1	<180	184	80	144	<100	88	80	192	4.3	(3)
27	19 Apr 72	LONGCHAMPS	EX 16 32 00	37°07.3'	116°05.0'	<1	70	280	20	72	70	112	100	350	4.2	(2)
28+	25 Jul 72		EX 13 30 00	36.9°	116.0°	<1	<10	24	<40	104	<10	40	56	214	4.0	(3)
29	26 Sep 72	DELPHINIUM	EX 14 30 00	37°07.3'	116°05.1'	<1	75	240							4.4	(2)
30	05 Aug 71		EQ 17 58 18	38°54.9'	115°59.6'	4.6	1040	60	800	160	1400	74	1300	192	4.2	(4)
31	05 Aug 71		EQ 22 20 03	36°53.6'	115°56.3'	9.0	40	7	34	44	48	25	42	15	3.3	(4)
32	18 Feb 73		EQ 18 05	36.9°	116.0°	?			78	60			120	40	3.8	(3)
33	19 Feb 73		EQ 11 15	36°49.0'	115°53.5'	4.7	92	45			80	40			3.9	(5)
34	19 Feb 73		EQ 13 43	36.9°	116.0°	?					80	28			3.5	(3)
35	20 Dec 68		EXA 20 08 19	37°13.0'	116°30.7'	4.1							144	40	4.1	(6)
36	21 Dec 68		EXA 00 14 25	37°15.8'	116°29.3'	3.5			320	136	592	136	800	296	4.8	(6)
37	22 Dec 68		EXA 18 10 52	37°14.2'	116°30.4'	4.3			90	56	90	89	320	104	4.2	(6)
38	06 Jan 69		EXA 06 34 15	37°14.7'	116°30.5'	4.2			400	300	208	88	800	216	4.6	(6)
39	10 Jan 69		EXA 08 08 41	37°10.8'	116°30.8'	7.1					26	7	120	20	3.6	(6)
40	10 Jan 69		EXA 09 81 22	37°10.8'	116°30.9'	2.7					120	48	880	176	4.6	(6)
41	10 Jan 69		EXA 17 01 45	37°10.6'	116°30.9'	2.8					128	40	440	56	4.4	(6)
42	10 Jan 69		EXA 17 14 17	37°11.1'	116°30.7'	3.0					80	32	320	114	4.5	(6)
43	27 Mar 70		EXA 15 45 06	37°18.4'	116°32.8'	3.6			20	7					3.5	(6)
44	16 Sep 69		C 15 43 39	37°18.8'	116°27.4'	.6(R)**							52	34	3.8	(6)
45	16 Sep 69		C 16 23 53	37°18.7'	116°27.3'	.6(R)					96	12	140	29	3.7	(6)
46	16 Sep 69		C 17 31 14	37°19.0'	116°27.4'	.6(R)					140	26	230	32	4.1	(6)
47	18 Sep 69		C 18 15 39.1	37°19.0'	118°27.3'	.6(R)					190	20	246	36	4.2	(6)
48	24 Mar 70		C 01 15	(SHAPER)					82	4	160	8	100	20	4.2	(3)
49	27 Mar 70		C 05 51	(HANDLEY)					240	44			100	48	3.8	(3)
50	27 Mar 70		C 16 42	(HANDLEY)					440	57	360	49	620	70	4.1	(3)
51	27 Mar 70		C 18 08	(HANDLEY)					1880	44	1400	56	960	88	4.2	(3)
52	27 Mar 70		C 18 18	(HANDLEY)					3200	320	3600	300	1440	800	4.9	(3)
53	15 May 70		C 15 20	(CORNICE)							280	10	280	112	3.6	(3)
54	08 Oct 71		C 15 33	(CATHAY)			160	40	140	80	90	35	90	164	4.3	(3)
55	25 Jul 72		C 13 54				32	8	21	32					3.2	(3)
56	26 Sep 72		C 15 25	(DELPHINIUM)					27	<3					2.8	(3)

Notes:

* Events not plotted in Figures 3-6.
** Restrained depth
\+ Presumed explosion

Data Sources
1. Springer and Kinnaman (1971)
2. PDE cards
3. Berkeley data
4. Fischer, Papanek, Hamilton (1972)
5. Fischer, personal communication, (1973)
6. Hamilton, Fischer, Papanek (1971)

Event type

EX = explosion
EQ = earthquake
EXA = explosion aftershock
C = collapse

TABLE 2. Regression Line Slopes and Standard Errors of Rayleigh wave versus P_n data Sets

Phase	Mina	Kanab	Landers	Berkeley	Springer & Hannon(1973)
PNMAX	1.16±.033(24)	1.14±.040(23)	1.33±.051(19)	1.38±.017(50)	1.51 *
PN 1	1.15±.040(23)	1.01±.045(19)	1.03±.047(17)		1.36 +

* Combination of four regional stations.

\+ Springer, personal communication (1973)

TABLE 3. Deviation in standard error units of the JORUM and HANDLEY data from the least squares lines of Table 2.

	PN1			PNMAX	
	JORUM	HANDLEY		JORUM	HANDLEY
MINA	1.09(3)	0.448(3)	MINA	3.34(1)	3.06(1.3)
KANAB	------	0.960(3)	KANAB	-----	3.13(3)
LANDERS	5.49(1)	3.52(1)	LANDERS	-0.815(1.3)	-0.892(.7)

TABLE 4. SOURCE PARAMETERS FROM SPECTRA.

Event No.	Station	Ω_p (cm-sec)	R(cm)	M_o (dyne-cm)	f_c (Hz)	r(km)	σ(bar)	Average M_o	M_L
	KANAB	1.11×10^{-4}	4.3×10^{7}	6.72×10^{22}	.52	3.9	.496	7.30×10^{22}	4.2
30	LANDERS	1.53×10^{-4}	4.4×10^{7}	9.49×10^{22}	.62	3.3	1.16		
	ELKO	8.11×10^{-4}	5.0×10^{7}	5.71×10^{22}	.42	5.0	.200		
36	MINA	3.97×10^{-4}	2.3×10^{7}	1.29×10^{23}	.60	3.3	1.57	8.23×10^{22}	4.8
	KANAB	7.41×10^{-5}	4.3×10^{7}	4.50×10^{22}	.61	3.4	.530		
	LANDERS	1.17×10^{-4}	4.4×10^{7}	7.29×10^{22}	.53	3.9	.538		
38	MINA	6.06×10^{-4}	2.3×10^{7}	1.97×10^{23}	.53	3.9	1.45	1.25×10^{23}	4.6
	KANAB	2.02×10^{-4}	4.3×10^{7}	1.23×10^{23}	.44	4.6	.553		
	LANDERS	8.73×10^{-5}	4.4×10^{7}	5.42×10^{22}	.74	2.8	1.08		
40	MINA	3.10×10^{-4}	2.3×10^{7}	1.01×10^{23}	.62	3.3	1.23	6.36×10^{22}	4.6
	LANDERS	4.24×10^{-5}	4.4×10^{7}	2.63×10^{22}	.44	4.6	.118		

FIGURE CAPTIONS

Figure 1. Stations of the LLL network (open triangles) and the Berkeley (BRK) observatory. Distances from NTS in km are shown in brackets.

Figure 2. Broadband displacement sensitivity curves, high gain channels, for LLL and BRK systems, using Berkeley playback system.

Figure 3, Rayleigh vs. P_n Amplitudes for events recorded at Elko, Nevada. Cuniforms denote upper limit readings.

Figure 4. Rayleigh vs. P_n Amplitudes for events recorded at Kanab, Utah. Cuniforms denote upper limit readings.

Figure 5. Rayleigh vs. P_n Amplitudes for events recorded at Landers, California. Cuniforms denote upper limit readings.

Figure 6. Rayleigh vs. P_n Amplitudes for events recorded at Mina, Nevada. Cuniforms denote upper limit readings.

Figure 7. Examples of P_g displacement spectra for non-explosion events used for source parameter determination by fitting spectra with solid lines as shown for corner frequency and DC level. The high frequency spectral roll-off is as frequency squared.

LAWRENCE LIVERMORE LABORATORY SEISMIC NETWORK

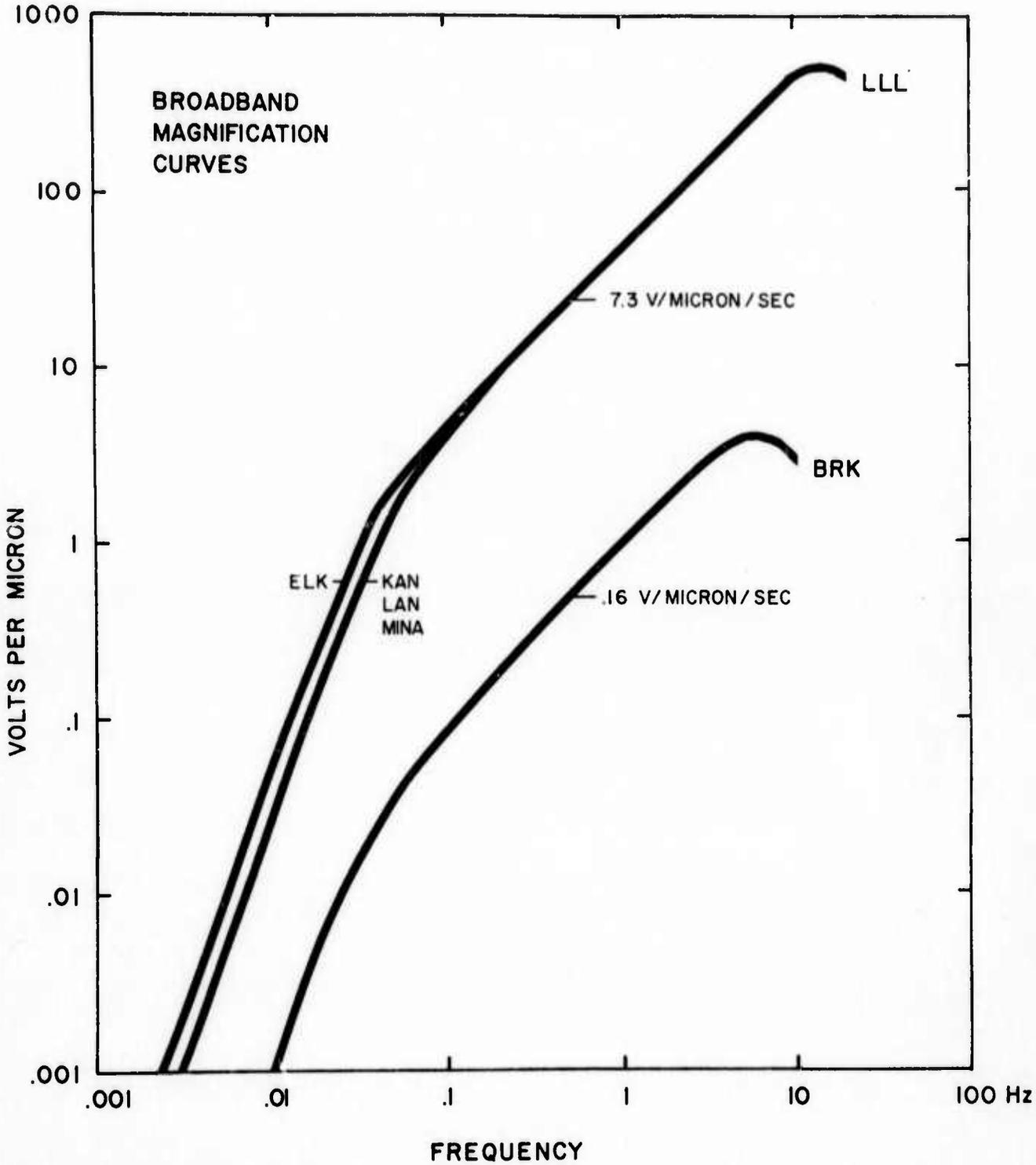
BROADBAND
MAGNIFICATION
CURVES
LLL
7.3 V/MICRON/SEC
BRK
.16 V/MICRON/SEC
ELK
KAN
LAN
MINA
1000
100
10
1
.1
.01
.001
VOLTS PER MICRON
.001
.01
.1
1
10
100 Hz
FREQUENCY

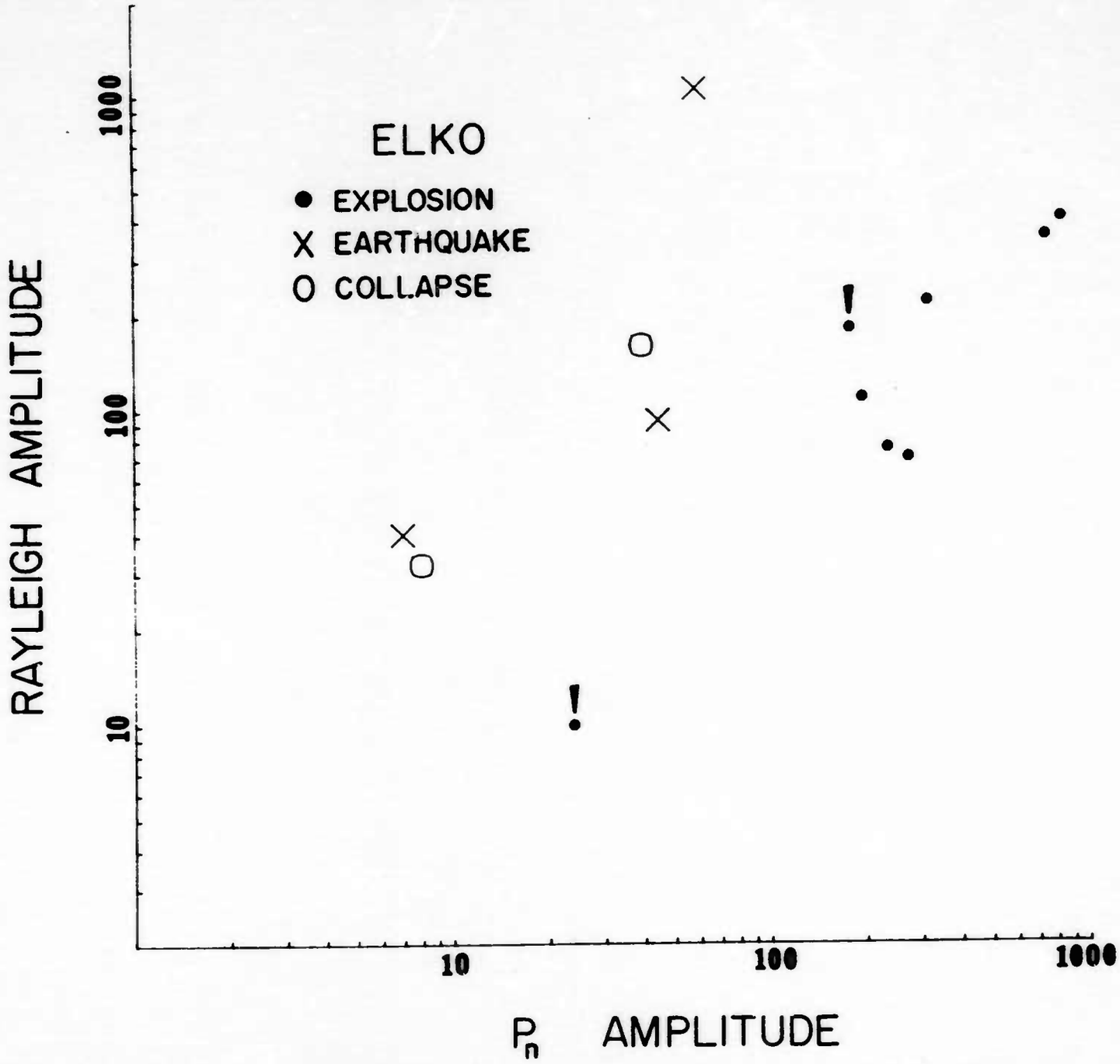
ELKO
● EXPLOSION
X EARTHQUAKE
O COLLAPSE
RAYLEIGH AMPLITUDE
1000
100
10
10
100
1000
P_n AMPLITUDE

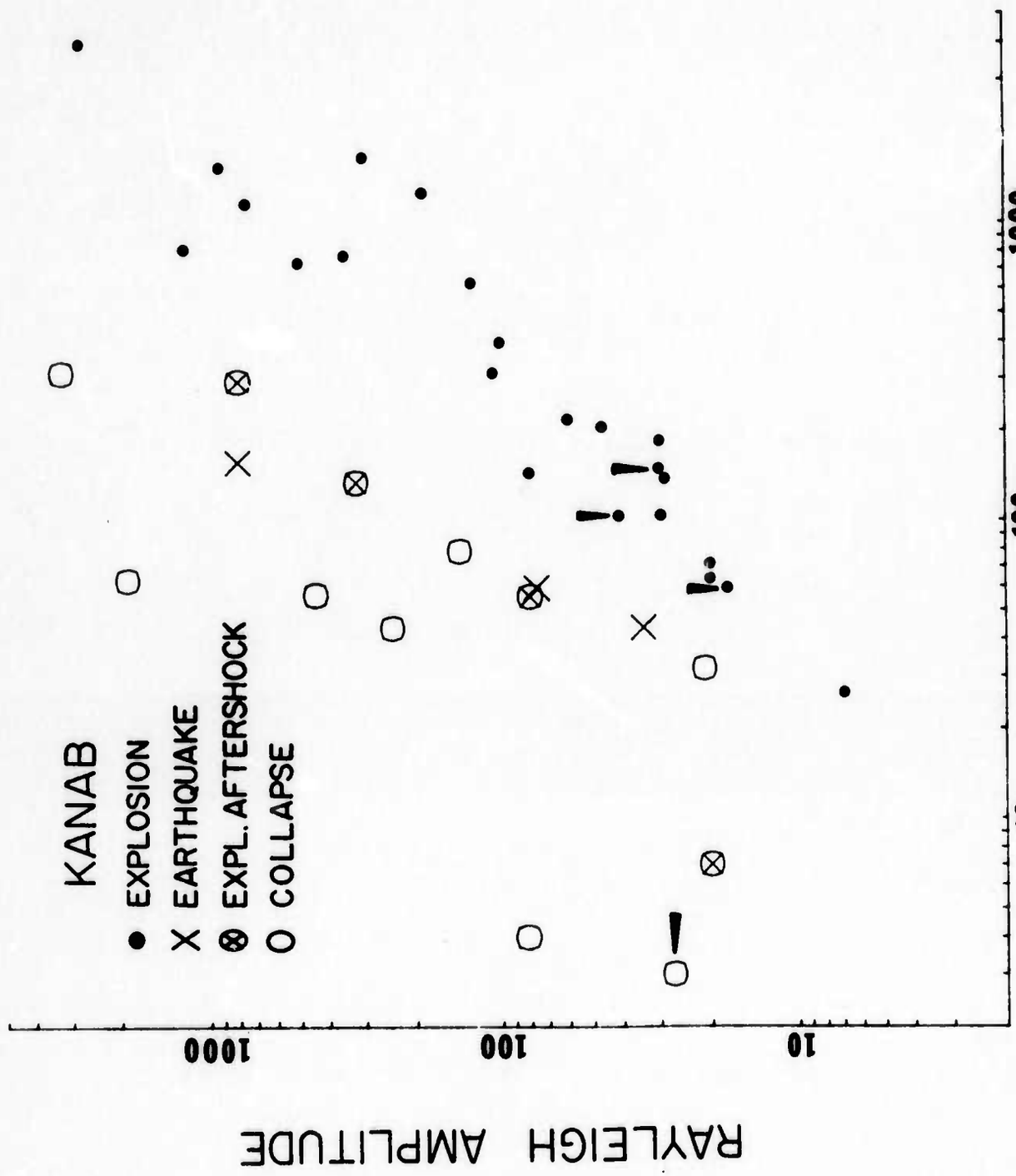
KANAB
EXPLOSION
EARTHQUAKE
EXPL. AFTERSHOCK
COLLAPSE
RAYLEIGH AMPLITUDE
1000
100
10
10
100
1000
P_n AMPLITUDE

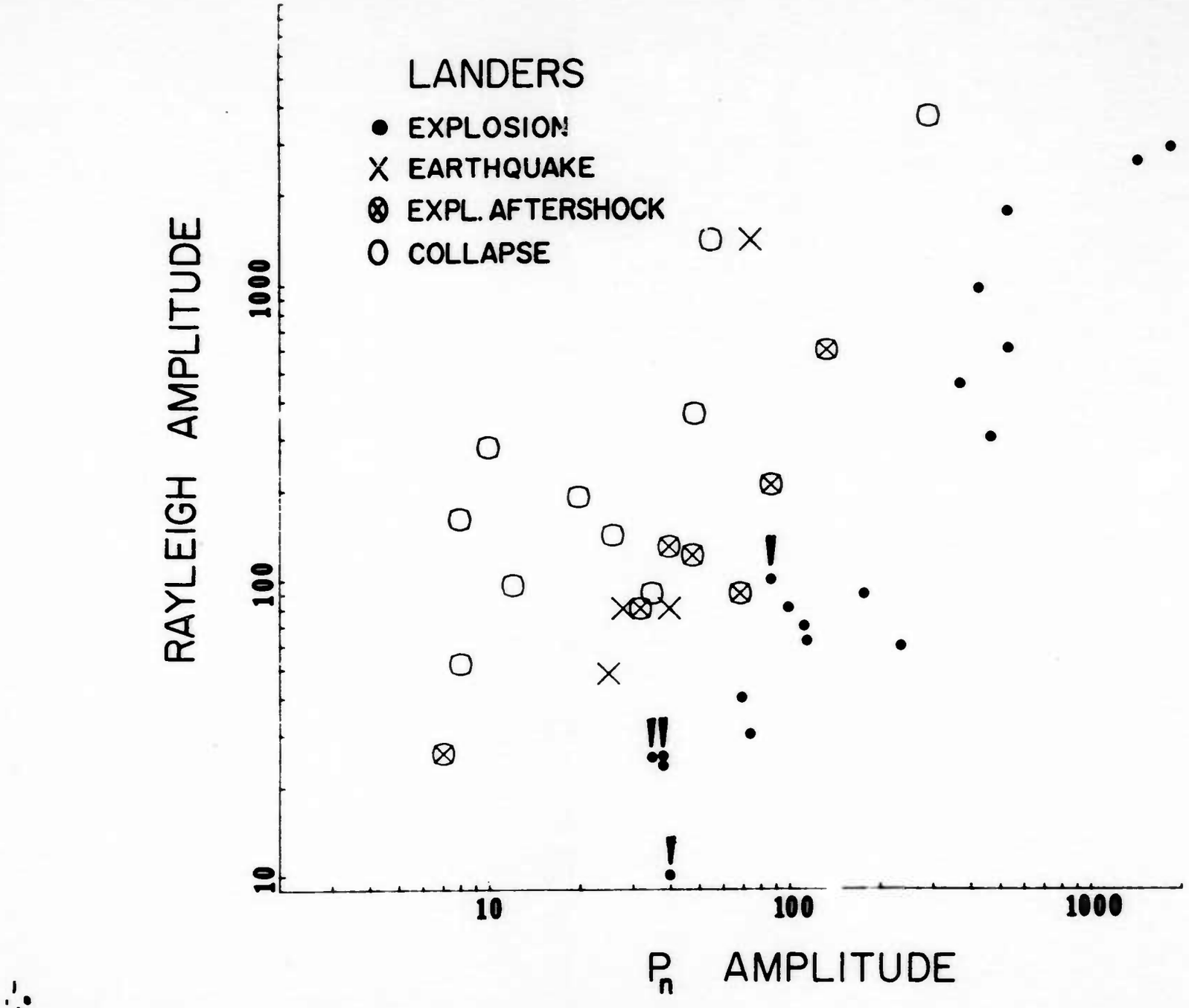
LANDERS
EXPLOSION
EARTHQUAKE
EXPL. AFTERSHOCK
COLLAPSE
RAYLEIGH AMPLITUDE
1000
100
10
10
100
1000
P_n AMPLITUDE

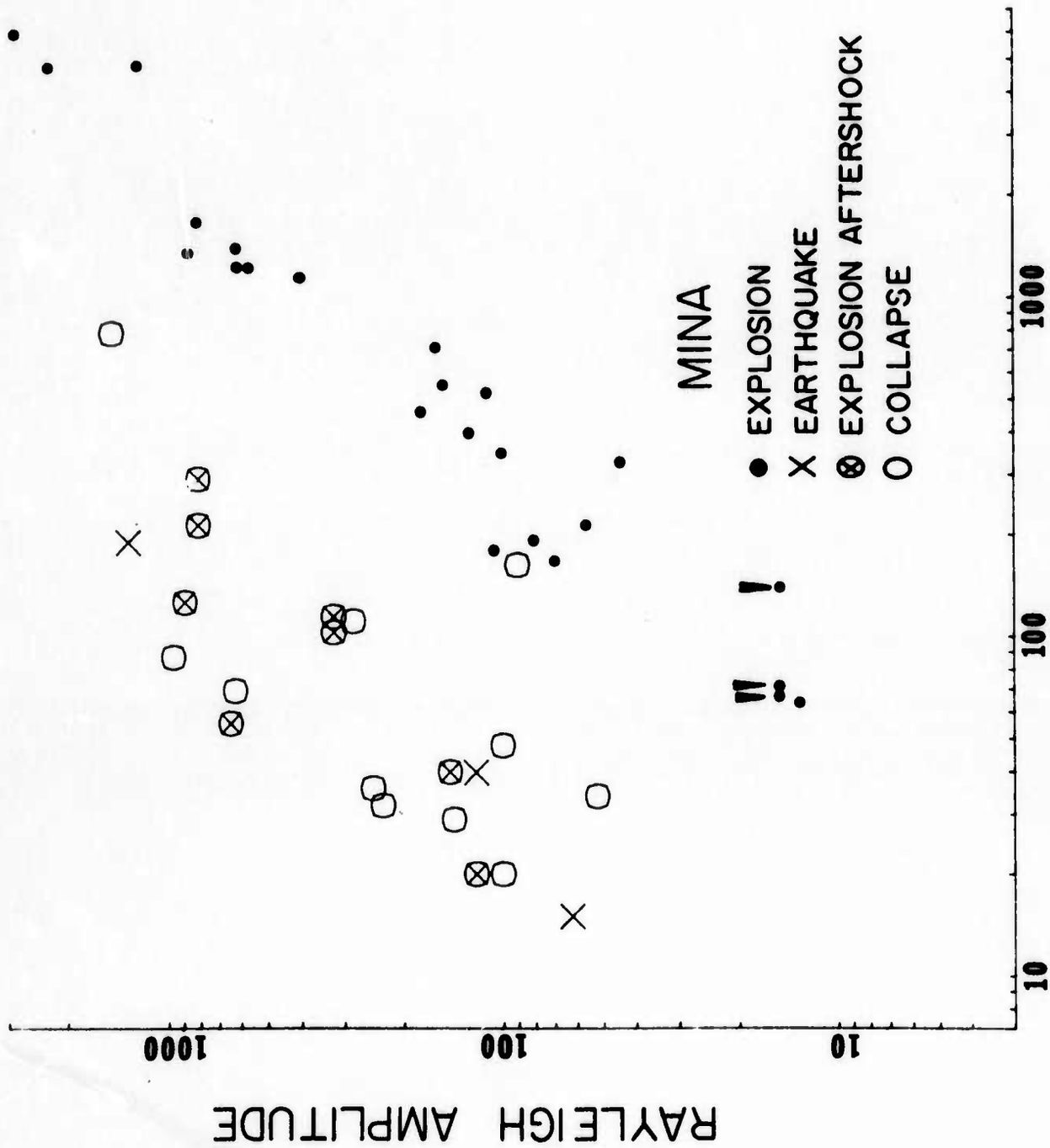
MINA
● EXPLOSION
X EARTHQUAKE
⊗ EXPLOSION AFTERSHOCK
O COLLAPSE
RAYLEIGH AMPLITUDE
1000
100
10
10
100
1000
P_n AMPLITUDE

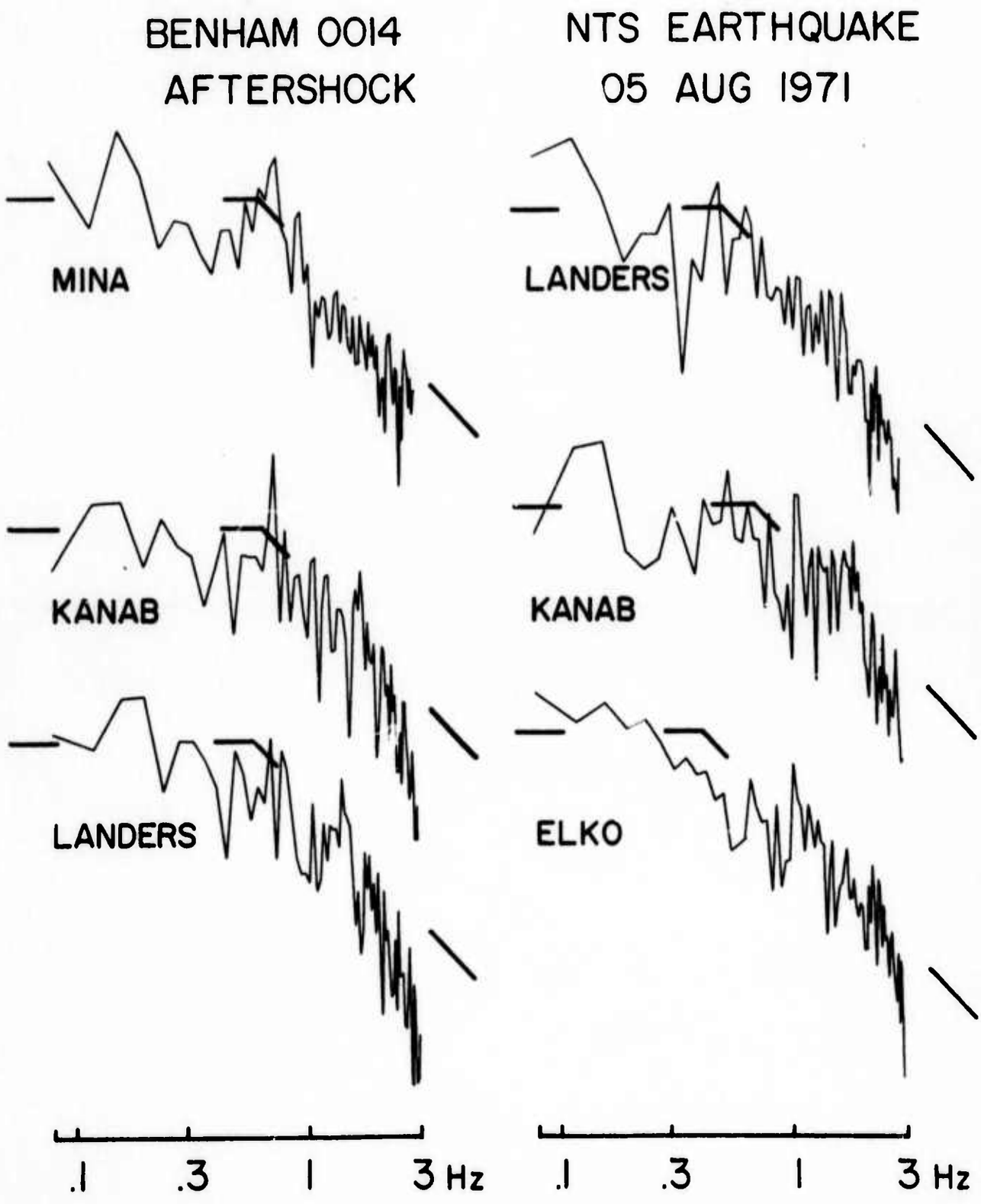
BENHAM 0014
AFTERSHOCK
NTS EARTHQUAKE
05 AUG 1971
MINA
KANAB
LANDERS
LANDERS
KANAB
ELKO
.1
.3
1
3 Hz
.1
.3
1
3 Hz